

Linking Soil O₂, CO₂, and CH₄ Concentrations in a Wetland Soil: Implications for CO₂ and CH₄ Fluxes

Bo Elberling,^{†,*} Louise Askaer,[†] Christian J. Jørgensen,[†] Hans P. Joensen,[†] Michael Kühl,^{‡,§} Ronnie N. Glud,^{||,⊥,#} and Frants R. Lauritsen[▽]

[†]Department of Geography and Geology, University of Copenhagen, Copenhagen, Denmark

[‡]Marine Biological Laboratory, Department of Biology, University of Copenhagen, Strandpromenaden 5, DK-3000 Helsingør, Denmark

[§]Plant Functional Biology and Climate Change Cluster, University of Technology, Sydney PO Box 123 Broadway NSW 2007 Australia

^{||}The Scottish Association for Marine Science, Dunstaffnage Marine Laboratory, Oban, Argyll, PA37 1QA, United Kingdom

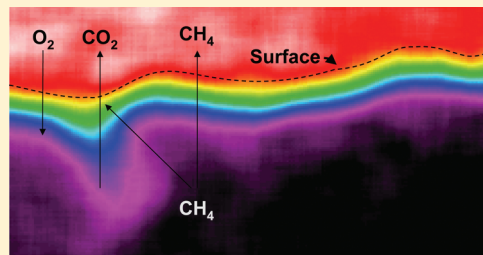
[⊥]Institute of Biology and Nordic Center for Earth Evolution, University of Southern Denmark, Odense M, Denmark

[#]Greenland Climate Research Centre, Kivioq 2, Box 570, 3900 Nuuk Greenland

[▽]Department of Pharmacy and Analytical Chemistry, University of Copenhagen, Universitetsparken 2, 2100 Copenhagen Ø, Denmark

Supporting Information

ABSTRACT: Oxygen (O₂) availability and diffusivity in wetlands are controlling factors for the production and consumption of both carbon dioxide (CO₂) and methane (CH₄) in the subsoil and thereby potential emission of these greenhouse gases to the atmosphere. To examine the linkage between high-resolution spatiotemporal trends in O₂ availability and CH₄/CO₂ dynamics in situ, we compare high-resolution subsurface O₂ concentrations, weekly measurements of subsurface CH₄/CO₂ concentrations and near continuous flux measurements of CO₂ and CH₄. Detailed 2-D distributions of O₂ concentrations and depth-profiles of CO₂ and CH₄ were measured in the laboratory during flooding of soil columns using a combination of planar O₂ optodes and membrane inlet mass spectrometry. Microsensors were used to assess apparent diffusivity under both field and laboratory conditions. Gas concentration profiles were analyzed with a diffusion-reaction model for quantifying production/consumption profiles of O₂, CO₂, and CH₄. In drained conditions, O₂ consumption exceeded CO₂ production, indicating CO₂ dissolution in the remaining water-filled pockets. CH₄ emissions were negligible when the oxic zone was >40 cm and CH₄ was presumably consumed below the depth of detectable O₂. In flooded conditions, O₂ was transported by other mechanisms than simple diffusion in the aqueous phase. This work demonstrates the importance of changes in near-surface apparent diffusivity, microscale O₂ dynamics, as well as gas transport via aerenchymous plants tissue on soil gas dynamics and greenhouse gas emissions following marked changes in water level.



INTRODUCTION

Northern wetlands store about 30% of the global subsurface organic carbon (C) pools and function as net sources of methane (CH₄) with an annual release of 46 Tg CH₄-C to the atmosphere.^{1–3} Soil water content is a key regulator for diffusion of O₂ into the soil. Lowering the water level increases the oxygen (O₂) availability in near-surface layers and accelerates decomposition rates of organic matter, increases carbon dioxide (CO₂) emissions, and decreases CH₄ emissions due to subsurface CH₄ oxidation. However, highly contrasting results in terms of the effects of lowered water levels on gas emission are reported in the literature and the controlling mechanisms are unclear.⁴ In particular, the temporal nature of the gas transport mechanism across the soil-atmosphere interface remains unresolved.^{5,6}

Subsurface O₂ concentrations in wetlands have rarely been reported at high spatiotemporal scales despite the fact that O₂ is a key parameter for the biogeochemistry of soils and sediments.

Subsurface O₂ concentrations can be quantified both in the laboratory and in situ with electrochemical and optical sensors.⁷ Most recently, 2D distributions of O₂ have been measured using planar optodes^{8–10} providing novel insights into high resolution O₂ dynamics in a range of complex and heterogeneous marine environments.⁹ In wetlands, detailed investigations on subsoil O₂ distribution are important as the transport of soil gases occurs both via diffusive transport in the pores as well as through the aerenchymous tissue of many wetland plants.^{11,12}

The quantification of soil-atmosphere gas exchange at a high spatiotemporal resolution requires detailed knowledge about the mass transfer properties of the soil system. However, standard

Received: October 20, 2010

Accepted: February 24, 2011

Revised: February 13, 2011

Published: March 17, 2011

equations for calculating effective diffusion coefficients of wetland soils and peat are few^{13,14} and limited by rapid changes in air-filled porosity as well as total porosity values following changes in water level. High resolution measurements of the mass transfer properties under fluctuating soil moisture conditions will potentially help clarifying the mechanisms regulating greenhouse gas emissions from wetland soils. Therefore, this work aims to (i) quantify subsurface O₂ dynamics in a protected Danish wetland with respect to natural water level fluctuations, and (ii) to quantify depth-specific O₂, CO₂, and CH₄ consumption/production profiles based on observed in situ gas concentrations and apparent gas diffusivity measurements using PROFILE, a simple diffusion-reaction model¹⁵ for analysis of measured concentration gradients.

MATERIALS AND METHODS

Study Site. The study site is situated in a temperate wetland area, Maglemeden (55°51'N, 12°32'E) formed through the retreat of an ancient inlet in Vedbæk, 20 km north of Copenhagen, Denmark (Supporting Information, SI, Figure 1S). Mean annual air temperature is 8 °C and mean annual precipitation is 613 mm (normals for 1961–1990, Danish Meteorological Institute). The wetland is characterized as a fen covering an area of roughly 0.6 km² with peat depths ranging from 0.5 to 3 m. The mean annual water level in 2007–2008 was 14 cm below the surface and ranged from 6 cm above the surface to 73 cm below the surface. The study site has not been managed for >100 years and is dominated by graminoids, mainly reed canary grass (*Phalaris arundinacea*) but also common reed (*Phragmites australis*) and different herbs.

Field Measurements and Sampling. Subsoil CO₂ and CH₄ concentration profiles and surface fluxes were measured on a weekly basis (January to August 2009). Ground temperature, water content, water level, and O₂ concentrations were logged continuously on an hourly basis. Soil CO₂ fluxes (microbial and root respiration) were measured using an infrared gas analyzer (LiCor 6400–09/6262 Soil CO₂ Flux Chamber, LiCor, Lincoln, USA) attached to a portable chamber, functioning as a dark and closed soil-flux chamber and placed on top of open preinstalled soil collars (10 cm in diameter) for 2–3 min at sites without plants within the collars. The CO₂ efflux was calculated on the basis of a linear increase ($r^2 > 0.95$) in chamber CO₂ concentrations over time on 10 replicate collars. Soil CH₄ fluxes were measured using three replicate static collars installed to a depth of 8 cm and leaving 2 cm above the surface. These collars were closed during measurements using a closed-end CHA-type plumbing creating a total chamber volume of about 0.5 L. Headspace gas samples were extracted four times at 15-min intervals and stored in 2.5 mL glass injection flasks with polyisobutylene septa. Gas samples were analyzed for CH₄ within 24 h using a gas chromatography (Shimadzu GC 2014 with Back Flush system, SHIMADZU EUROPA GmbH, Duisburg, Germany) equipped with a Mol Sieve 5A 80/100 mesh (1/8" × 1 m) column connected to an FID detector.

Air in the soil pores was sampled for CO₂ and CH₄ analyses at depths of 5, 10, 20, 30, 40, 50, 60, 80, 110, and 140 cm using silicone probes as described.^{16,17}

Oxygen (O₂) concentrations were measured at in situ 5, 10, 15, 20, 25, 30, 40, 50, 60, 80, and 110 cm depth using fiber-optic O₂ optodes connected to a fiber-optic oxygen meter (FIBOX 3, Presens GmbH, Germany) in combination with K-type

thermocouples connected to a thermometer (RS 206–3722). Temperature readings were made with the same spatiotemporal resolution as O₂ in order to enable temperature compensation of the sensor signals. All sensors were linearly calibrated with a 2 point temperature and O₂ concentration procedure with precisions $\leq 5\%$ of standard deviation at standard temperature and pressure. In the laboratory, electrochemical O₂ microsensors (OX-50, 40–60 μm tip diameter; Unisense A/S, Aarhus, Denmark) connected to a pA meter (PA2000, Unisense A/S, Aarhus, Denmark) were used to measure O₂ concentrations under flooded conditions with O₂ penetration depths were <5 cm and in soil without plants (>0.5 m from nearest *Phalaris arundinacea*).

Volumetric soil water content was measured using soil moisture sensors (Theta Probes ML2x, Delta-T Devices Ltd., Cambridge, UK) installed in 8 depths in one profile and connected to a datalogger (Campbell, CR10X Datalogger for Measurement & Control, Campbell Scientific Ltd., Loughborough, UK). The water level was measured by a pressure sensor (PCR 1830, Druck) submerged in a 2.5 m perforated plastic tube. All installations were completed more than two months prior to measurements (see SI).

Depth and volume-specific soil samples ($\sim 100 \text{ cm}^3$) were collected from pits and included all major horizons (including the litter layer). In situ pH measurements (Metrohm 704 Pocket pH meter, Metrohm Nordic, Glostrup, Denmark) were made directly with probes inserted into peat/sediment or after the addition of distilled water at depths with a soil-solution ratio of $\sim 1:2.5$. Bulk density was determined on the basis of the weight of dried volume-specific soil cores. Total organic carbon (TOC) was measured after acidification, using 6 M HCl to remove inorganic C using an Eltra SC-500 analyzer (ELTRA GmbH, Neuss, Germany), with an accuracy of $\pm 0.2\%$. Four replicate soil columns were sampled and stored in the dark at 4 °C until analysis in the laboratory. Three additional columns without living plants were sampled during winter in circular PVC columns (id:20 cm, h:60 cm), with one side removed, where a Plexiglas sheet containing a planar optode was fixed for laboratory experimental work. The soil column openings were closed with rubber-coated aluminum sheets, the upper with a large opening to ensure equilibrium with the atmosphere.

Experimental Work. Gas profiling using Membrane Inlet Mass Spectrometry (MIMS) and planar optode (PO) imaging were made in the dark at 10 °C after >6 months preincubation to obtain steady state conditions, and with a water level 5 cm above the peat surface. An aquarium pump was used to aerate the water column keeping it at atmospheric O₂ saturation. Depth-specific analyses of dissolved CH₄, CO₂, and Ar concentrations were done with a quadrupole mass spectrometer (QMA125, Balzers, Liechtenstein), where CH₄ and CO₂ concentrations were normalized using a two-point calibration with Ar as an internal standard. Details of the MIMS and PO setups have been described elsewhere¹⁷ and are also included in the SI.

Apparent Diffusivity. Microscale diffusivity sensors (DF200, Unisense A/S, Aarhus, Denmark) with a tip diameter of 200 μm were applied to measure apparent diffusivity, i.e., the bulk diffusivity in partly saturated peat and sediment by measuring concentrations of a tracer gas in an internal H₂ gas (at 1 atm partial pressure) reservoir within the sensor tip.¹⁸ In brief, the diffusivity sensor is a hydrogen transducer in which an air volume behind a separating membrane is continuously flushed avoiding potential interference with both O₂ and CO₂. A mathematical model has been made¹⁸ which describes the sensor signal as a

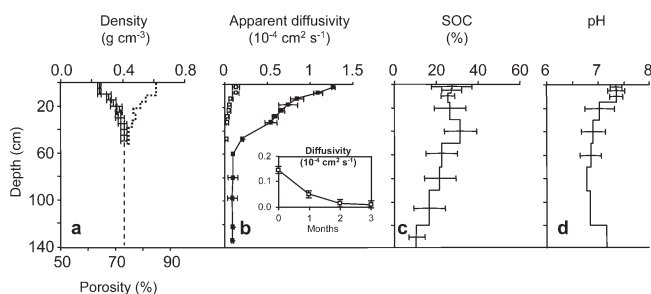


Figure 1. Depth specific soil properties including (a) bulk density (solid line) and porosity (dashed line) down to 50 cm; (b) in situ apparent O_2 diffusivity measured under saturated conditions (open squares) and well-drained conditions (filled squares); and (c) soil organic C, (d) in situ soil pH. Bars represent one standard deviation ($n = 4$). Insert in part b shows the changes in apparent O_2 diffusivity measured in well-drained top peat samples (0–3 cm, $n = 5$) over 3 months following flooding under laboratory conditions.

function of diffusivity and is based on a two-point calibration. Standards for calibration in this work included: (1) stagnant water, (2) 5–20 and 40–75 μm unsorted glass beads in water, and (3) a standard moist peat sample. The apparent diffusivity of the glass beads have previously been measured in diffusion chambers¹⁸ and the moist peat sample was previously measured.¹⁹ In the current study, mean values ($n = 25$) of apparent diffusivity for each depth interval was measured in situ under drained condition. Measurements were repeated in the laboratory using intact cores and subsequently measured again after flooding (within one week). Measurements were repeated monthly on 5 replicate cores from the well-drained top layer monthly over 3 months following core flooding. Tabulated values for the O_2 solubility and diffusion coefficient²⁰ were used to calculate O_2 concentrations at atmospheric saturation and the diffusivity of O_2 in distilled water at 10 °C ($1.57 \times 10^{-5} \text{ cm}^2 \text{ s}^{-1}$). Diffusion coefficients for CO_2 and CH_4 were calculated by multiplying the value for O_2 by 0.7961 and 0.8495.^{20,21}

Oxygen Diffusion-Reaction Model. Steady-state profile analysis was performed using the diffusion-reaction model PROFILE¹⁵ providing estimates of net consumption/production rates as a function of depth using measured diffusivities and gas concentrations as input values. The diffusion-reaction model provides an objective selection of the simplest consumption/production profile that reproduces the measured concentration profiles based on Ficks' second law. On the basis of such calculated production/consumption profiles, the depth-integrated gas fluxes were estimated by PROFILE and subsequently compared to fluxes measured in situ. Boundary conditions for simulations were no flux at the bottom and atmospheric conditions at the top.

RESULTS AND DISCUSSION

Site Characteristics. The wetland soil profile (SI Figures 2S, 3S) can be divided into three functional layers: A top surface 10 cm layer with recently deposited organic C with a bulk density of 0.2–0.3 g cm^{-3} , a mean pH of 7.3 and a mean organic C content of 28% (Figure 1). From 10 to 50 cm, the bulk density increases to about 0.4 g cm^{-3} and pH values decrease to 7. The amount of organic C within the upper 30 cm (main root zone) is 29 kg m^{-3} . Below 50 cm depth, the sediment is dominated by brackish lake sediments with a decreasing organic C content.

Apparent Diffusivity. Apparent diffusivities measured in situ and in the laboratory (SI Figure 4S) show similar results indicating

that intact cores can be moved to the laboratory and used to represent the apparent diffusivity in the field. However, apparent diffusivity measurements across intact cores need to be made in steps to identify “edge effects” (SI Figure 5S). Extreme values in the boundary zones of ~ 0.5 cm from the top/bottom indicate the physical limitation of laboratory diffusion measurements using intact cores.

Apparent diffusivity measurements (Figure 1b) normalized to 10 °C show values in newly saturated peat layers about 10 times the diffusivity in water ($1.57 \times 10^{-5} \text{ cm}^2 \text{ s}^{-1}$). This is in line with previous reported peat diffusivities¹³ and is considered a result of a small but continuous soil–air network. Repeated laboratory measurements over 3 months following saturation ($n = 5$) showed that the apparent diffusivity decreased slowly by a factor of 8 (Figure 1b, insert). These changes over time occur as trapped soil air is replaced by water, decreasing the gas phase volume and/or generating less connected air spaces in the peat matrix. Similar changes have been observed for water retention caused by “wetting inhibition”,²² where the phenomenon is explained by a combination of air inclusion, water-repelling films, and pore geometry alterations due to shrinkage during drying. Repeated measurements of such time-dependent changes in apparent diffusivity (Figure 1b, insert) also indicated that also the degree of drainage before flooding is important. Longer and more extensive drainage resulted in higher apparent diffusivities upon flooding and a longer time (weeks to months) was required to reach a constant apparent diffusivity (data not shown).

Laboratory manipulations of the water level showed a marked increase in soil fauna activity following flooding. Newly created macropores for air and water flow by migrating earthworms in the top 10 cm add to the complexity of mass transfer in the peat soil.¹⁷

The combination of the above observations leads us to conclude that the position of the water level and water content measurements are inadequate predictors of temporal changes in the apparent diffusivity. Even minor changes in air-filled and total porosities following physical shrinkage or swelling of the peat can over time change the apparent diffusivity by a factor 8 after flooding.

Temporal Variations in Gas Concentrations and Fluxes. Measurements from January to August 2009 showed fluctuating water levels from intermittent flooding during winter followed by a general water level drawdown during summer with some interference from precipitation events (Figure 2). Water saturation followed the same pattern but remained high (>80% by saturation) throughout the summer. During winter, ground temperatures were 0–4 °C and despite flooded conditions, O_2 was present in the upper 10 cm at sites with vegetation (Figure 2). In contrast, experimental work without plants showed O_2 depletion within the upper 4 mm (Figure 3a). Due to warm summer air temperatures and low water levels, temperatures reached 16–20 °C in the top 30 cm and O_2 levels were up to 80% air saturation within the top 40 cm. Generally, concentrations of CO_2 and CH_4 varied markedly over the time period with warmer conditions leading to increasing concentrations of CO_2 above the water level and CH_4 concentrations below the water level (Figures 2 and 3). During flooded conditions (March 3, 2009), CO_2 and CH_4 concentrations increased with depth to 3000 and 150 μM , respectively (Figure 3A). Comparable concentration ranges have previously been reported from similar sites.²³ Fluxes of CO_2 and CH_4 were low in winter and increased with temperature until the early part of the growing season when near-surface oxic conditions further increased CO_2 fluxes but limited CH_4 fluxes. When the water level was below 40 cm, the CH_4 flux was negative indicating a net

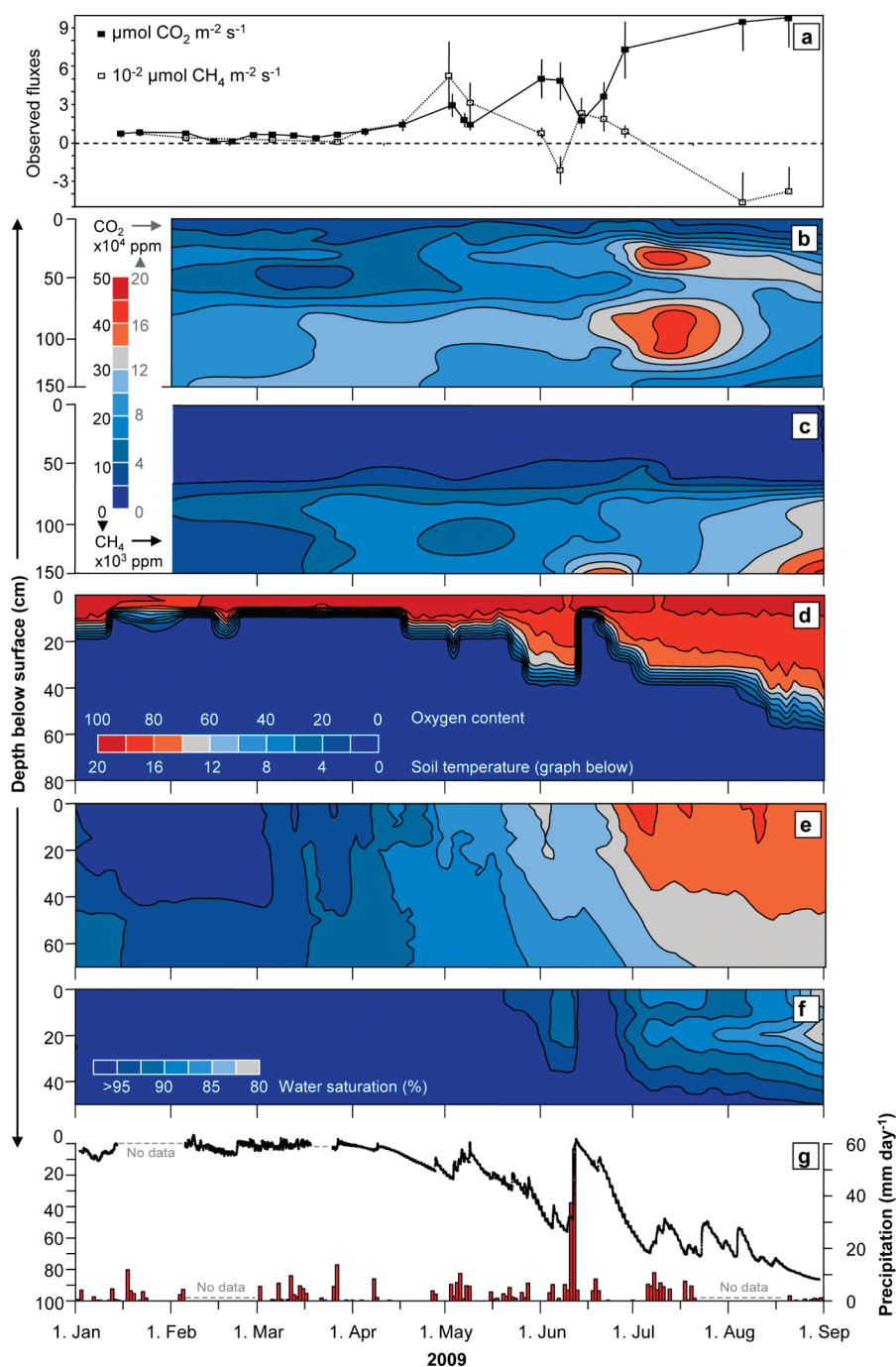


Figure 2. Temporal changes in subsurface conditions from January through August 2009; (a) weekly observed CO₂ and CH₄ fluxes; (b) subsurface CO₂ concentrations; (c) subsurface CH₄ concentrations; (d) subsurface O₂ concentrations (% air saturation); (e) ground temperatures ($^{\circ}\text{C}$); (f) water contents (% saturation); and (g) water level (shown as a line) and daily precipitation (shown as bars).

uptake. These shifts in CO₂ and CH₄ fluxes and the magnitude of fluxes are within the range quantified in other Northern wetlands.³

Modeling Soil Gas Dynamics during Steady State Field Conditions. Concentration profiles were analyzed within two time frames assuming steady-state conditions; after months with the water level above the ground surface (0–5 cm) and after weeks with the water level fluctuating below 50 cm (Figure 2). Modeled production and consumption profiles showed that CO₂ and CH₄ were mainly produced within the upper 20 cm containing newly deposited organic material and the main rhizosphere

zone. However, these rates are lower than those reported from similar wetlands.² The CH₄ production profile could also be influenced by different CH₄ production pathways, i.e., near-surface acetate fermentation versus deeper methanogenesis from the reduction of CO₂ in less reactive layers.²³ We found maximum CH₄ in situ fluxes of $0.005 \mu\text{mol CH}_4 \text{ m}^{-2} \text{ s}^{-1}$, which were very low as compared to potential CH₄ production rates observed in laboratory studies, i.e., $0.01–10 \mu\text{mol CH}_4 \text{ m}^{-3} \text{ s}^{-1}$.²⁴

After a period of natural drainage and water level depths >50 cm (August 20, 2009), O₂ was present to a depth of 50 cm

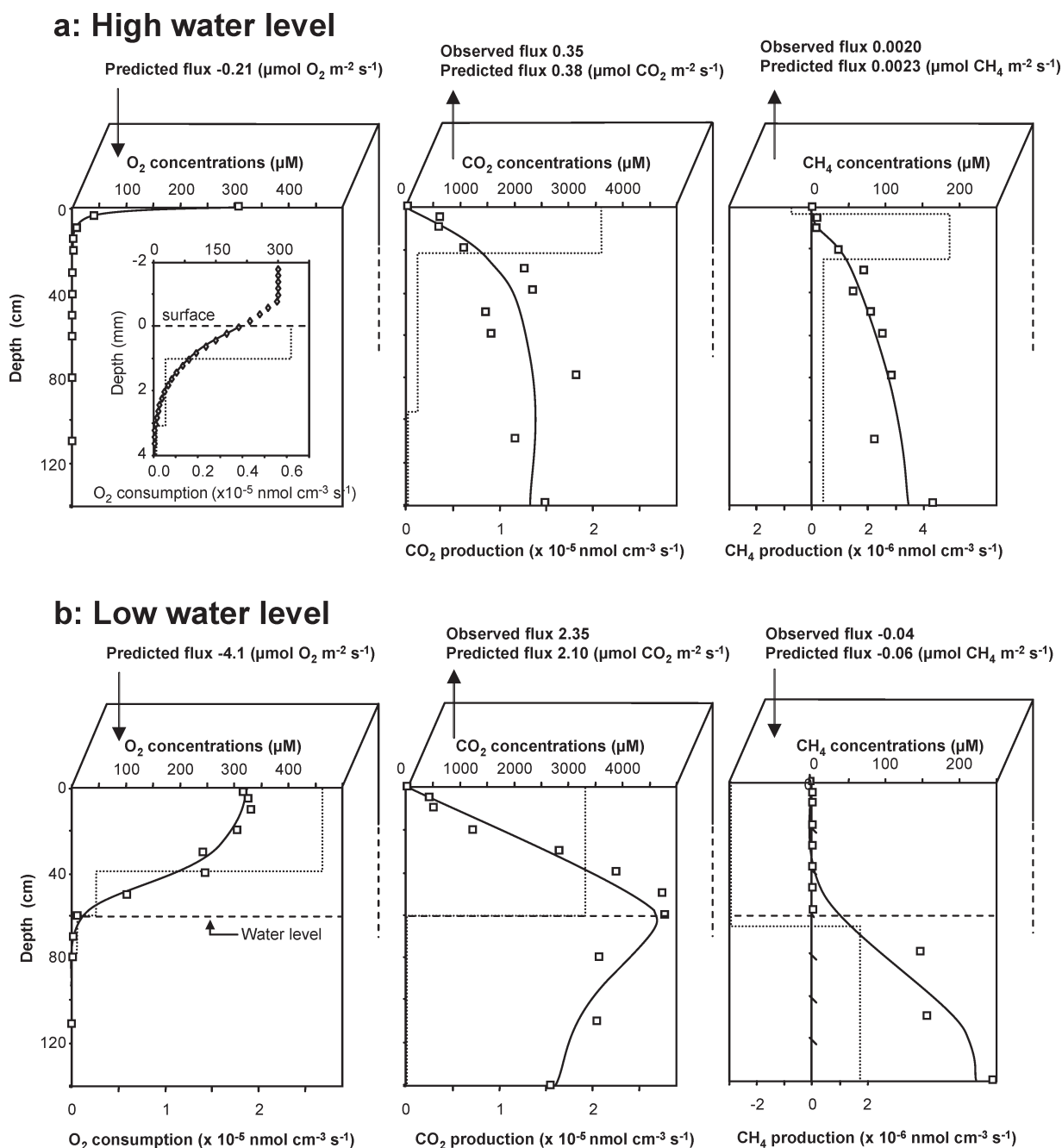


Figure 3. Field observed (symbols) and simulated (lines) subsurface gas concentrations at near steady state conditions: (a) cold and flooded conditions on March 20, 2009 and (b) warm and water level below 50 cm on August 20, 2009. Consumption and production profiles (dashed lines) are made using PROFILE (see Materials and Methods) and the depth-integrated net uptake or release of CO_2 and CH_4 are compared to in situ observed fluxes. Under flooded conditions, O_2 is measured using microsensors (diamonds) and under drained conditions O_2 is measured using optodes (squares).

and the O_2 flux (based on PROFILE simulation) was 20 times larger than under flooded conditions. Corresponding maximal CO_2 concentration (about $4500 \mu\text{M}$) was also observed at 50 cm depth (Figure 3B). The total subsurface O_2 flux ($\sim 4 \mu\text{mol O}_2 \text{ m}^{-2} \text{ s}^{-1}$) was almost twice as high as the total surface CO_2 flux according to PROFILE simulations. This could be caused by a notable amount of CO_2 being dissolved in the liquid phase and transported out of the soil-ecosystem without being released to the atmosphere, in line with previous observations²⁵ and high dissolved C export rates from wetlands which is an advective transport not represented in our profiles of transport coefficients.²⁶ CH_4 concentrations increased from

atmospheric levels above the water level to $>100 \mu\text{M}$ with increasing depth. However, concentrations and production rates cannot be directly compared as the flooded conditions typically occurred during winter with low temperatures, while the drained conditions occurred during summer with markedly warmer temperatures (Figure 2). Rates estimated from our PROFILE analysis were depth-integrated and compared with observed surface fluxes in situ (Figure 3) showing reasonable agreement between observed and modeled fluxes.

Laboratory Experiment. Laboratory measurements of O_2 by planar optode and CO_2/CH_4 using a MIMS (Figure 4 and SI Figure 6S) were performed to provide data for controlled steady

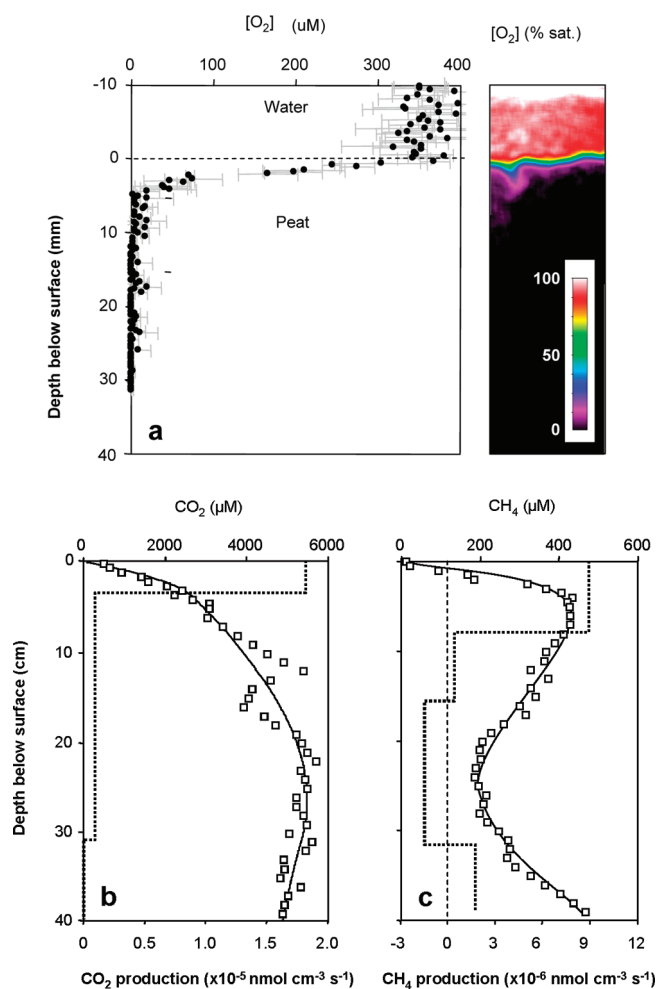


Figure 4. Laboratory observed (symbols) and simulated (lines) subsurface gas concentrations: (a) An image of the O₂ distribution using planar optodes and the mean O₂ concentration (\pm one standard deviation) across the entire image, (b) subsurface CO₂ concentrations, and (c) subsurface CH₄ concentrations measured by MIMS. Consumption and production profiles (dashed lines) were made using PROFILE.

state conditions and to explore links between often reported one-dimensional gas gradients and area-based flux measurements. After more than 6 months of dark incubation at 10 °C, O₂ penetrated down to about 4 mm (Figure 4 and SI Figure 7S) similar to results from in situ measurements in soil without active plant growth. Subsurface concentrations of both CO₂ and CH₄ were high: >5000 μ M CO₂ and >400 μ M CH₄ but also highly variable with depth. We speculate that such variations, particularly at 10–30 cm depth, were influenced by dead but open culms of grasses.²⁷ The flux of CH₄ calculated from PROFILE was 0.10 μ mol CH₄ m⁻² s⁻¹, which is about twice the mean value of measured fluxes using flux chambers in the laboratory (0.065 μ mol CH₄ m⁻² s⁻¹). This can originate in uncertainties related to the PROFILE simulations or that some CH₄ oxidation occurred in the well-oxidized water/sediment interface, which is not reflected in the relatively coarse depth resolution of the field profiles and consequently not accounted for in PROFILE.

We attribute the higher concentrations of CH₄ (and higher fluxes) measured under flooded laboratory conditions as opposed to flooded field conditions to be due to a combination of slightly

warmer conditions as well as the absence of plants in the laboratory experiment. Although plant activity is low during the initial growth stage in March, seedlings of *Phalaris arundinacea* with internal aeration through aerenchymous tissue^{28–30} start to develop under complete water covered conditions (anoxia).

CONCLUSIONS

This work focused on the diffusive gas dynamics in the soil air and pore water phases, which both affect the net fluxes of CO₂ and CH₄ across the soil–atmosphere interface. Our study suggests that the near-surface O₂ level is affected by transport linked to the presence of plants and O₂ release from plant roots. Analysis of concentration gradients showed that CH₄ oxidation can occur below the water level both under completely flooded conditions as well as for conditions with the water level well below the surface (Figure 3). The immediate oxidation of CH₄ by O₂ near the roots may explain our finding of rather low CH₄ emissions rates to the atmosphere through the bulk soil matrix, indicating that gas transport through plants is an important control on the overall CH₄ budget. Direct measurement of ecosystem CH₄ emissions in dynamic chambers suggest that roughly 80% of the total CH₄ emission at the actual study site can be mediated through plants. We conclude that the linkage between subsurface gas concentrations and surface fluxes can be roughly predicted by simple gas diffusion, but only if soil and depth specific apparent diffusivities are taken into account. We have shown that microscale patterns in time and space are more important than reported so far. In particular, this work highlights the importance of changes in near-surface time-dependent apparent diffusivity following flooding and the influence of macro fauna activity. Future measurements should include the entire ecosystem (including plants and macro fauna) as well as further studies of the microscale O₂ distribution in order to improve the quantification of processes linking subsurface greenhouse gas production and net gas emissions in wetlands with marked water level variations not least in a climate change context.

ASSOCIATED CONTENT

Supporting Information. Seven figures provide additional information about the field site and the experimental setup. This material is available free of charge via the Internet at <http://pubs.acs.org>.

AUTHOR INFORMATION

Corresponding Author

*Phone: (+45) 3532 2520; e-mail: be@geo.ku.dk.

ACKNOWLEDGMENT

This work was conducted within the framework of the project “Oxygen Availability Controlling the Dynamics of Buried Organic Carbon Pools and Greenhouse Emissions” financed by the Danish Natural Science Research Council (PI: B.E.). We wish to thank Lars Rickelt for constructing the planar optodes and for many valuable discussions, to Gry Lyngsø and Louise Langhorn for help with fieldwork, sample collection, and laboratory analysis and very helpful journal review comments.

REFERENCES

(1) Gorham, E. Northern peatlands: Role in the carbon cycle and probable responses to climatic warming. *Ecol. Appl.* **1991**, *1*, 182–195.

- (2) Blodau, C.; Moore, T. R. Micro-scale CO₂ and CH₄ dynamics in a peat soil during a water fluctuation and sulphate pulse. *Soil Biol. Biochem.* **2003**, *35*, 535–547, DOI: 10.1016/S0038-0717(03)00008-7.
- (3) Strack, M.; Waddington, J. M. Response of peatland carbon dioxide and methane fluxes to a water table drawdown experiment. *Global Biogeochem. Cycles* **2007**, *21*, GB1007, DOI: 10.1029/2006GB002715.
- (4) Laiho, R. Decomposition in peatlands: Reconciling seemingly contrasting results on the impacts of lowered water levels. *Soil Biol. Biochem.* **2006**, *38*(8), 2011–2024, DOI: 10.1016/j.soilbio.2006.02.017.
- (5) Wachinger, G.; Fiedler, S.; Zepp, K.; Gättinger, A.; Sommer, M.; Roth, K. Variability of soil methane production on the micro-scale: Spatial association with hot spots of organic material and Archaeal populations. *Soil Biol. Biochem.* **2000**, *32*, 1121–1130, DOI: 10.1016/S0038-0717(00)00024-9.
- (6) Le Mer, J.; Roger, P. Production, oxidation, emission, and consumption of methane by soils: A review. *Eur. J. Soil Sci.* **2001**, *37*, 25–50, DOI: 10.1016/S1164-5563(01)01067-6.
- (7) Kühn, M. Optical microsensors for analysis of microbial communities. *Environmental Microbiology. Methods Enzymol.* **2005**, *397*, 166–199, DOI: 10.1016/S0076-6879(05)97010-9.
- (8) Glud, R. N.; Ramsing, N. B.; Gundersen, J. K.; et al.; Planar optodes, a new tool for fine scale measurements of two-dimensional O₂ distribution in benthic communities. *Mar. Ecol.: Prog. Ser.*, **1996**, *140*, 217–226; IDS Number: VJ377.
- (9) Glud, R. N. Oxygen dynamics of marine sediments. *Mar. Biol. Res.* **2008**, *4*, 243–289, DOI: 10.1080/17451000801888726.
- (10) Kühn, M.; Polerecky, L. Functional and structural imaging of phototrophic microbial communities and symbioses. *Aquat. Microb. Ecol.* **2008**, *53*, 99–118, DOI: 10.3354/ame01224.
- (11) Armstrong, W. Oxygen diffusion from the roots of some British bog plants. *Nature* **1964**, *204*, 801–802.
- (12) Colmer, T. D. Long-distance transport of gases in plants: a perspective on internal aeration and radial oxygen loss from roots. *Plant, cell Environ.* **2003**, *26*(1), 17–36.
- (13) Stephen, K. D.; Arah, J. R. M.; Thomas, K. L.; Benstead, J.; Lloyd, D. Gas diffusion coefficient profile in peat determined by modelling mass spectrometric data: implications for gas phase distribution. *Soil Biol. Biochem.* **1998**, *30*(3), 429–431, DOI:10.1016/S0038-0717(97)00118-1.
- (14) Iiyama, I.; Hasegawa, S. Gas diffusion coefficient of undisturbed peat soils. *Soil Sci. Plant Nutr.* **2005**, *51*(3), 431–435, DOI: 10.1111/j.1747-0765.2005.tb00049.x.
- (15) Berg, P.; Risgaard-Petersen, N.; Rysgaard, S. Interpretation of measured concentration profiles in sediment pore water. *Limnol. Oceanogr.* **1998**, *43*, 1500–1510.
- (16) Kammann, C.; Grunhage, L.; Jäger, H.-J. A new sampling technique to monitor concentrations of CH₄, N₂O and CO₂ in air at well-defined depths in soils with varied water potential. *Eur. J. Soil Sci.* **2001**, *52*, 297–303, DOI: 10.1046/j.1365-2389.2001.00380.x
- (17) Askaer, L.; Elberling, B.; Glud, R. N.; Kühn, M.; Lauritsen, F. R.; Joensen, H. P. Soil heterogeneity effects on O₂ distribution and CH₄ emissions from wetlands: In situ and mesocosm studies with planar O₂ optodes and membrane inlet mass spectrometry. *Soil Biol. Biochem.* **2010**, *42*, 2254–2265, DOI: 10.1016/j.soilbio.2010.08.026.
- (18) Revsbech, N. P.; Nielsen, L. P.; Ramsing, N. B. A novel microsensor for determination of apparent diffusivity in sediments. *Limnol. Oceanogr.* **1998**, *43*, 986–992.
- (19) Elberling, B. Gas phase diffusion coefficients in cemented porous media. *J. Hydrol.* **1996**, *178*, 93–108.
- (20) Ramsing, N.; Gundersen, J. Seawater and gases—Tabulated physical parameters of interest to people working with microsensors in marine systems. Version 2.0. 1994, Unisense Internal Report, 16 pp.
- (21) Li, Y.-H.; Gregory, S. Diffusion of ions in seawater and deep-sea sediments. *Geochim. Cosmochim. Acta* **1974**, *38*, 703–714.
- (22) Schwärzel, K.; Renger, M.; Sauerbrey, R.; Wessolek, G. Soil physical characteristics of peat soils. *J. Plant Nutr. Soil Sci.* **2002**, *165*(4), 479–486, DOI: 10.1002/1522-2624(200208).
- (23) Hornibrook, E. R. C.; Longstaff, F. J.; Fyfe, W. S. Spatial distribution of microbial methane production pathways in temperate zone wetland soils: Stable carbon and hydrogen isotope evidence. *Geochim. Cosmochim. Acta* **1997**, *61*, 745–753, DOI: 10.1016/S0016-7037(96)00368-7.
- (24) Segers, R. Methane production and methane consumption: A review of processes underlying wetland methane fluxes. *Biogeochem.* **1998**, *41*, 23–51, DOI: 10.1023/A:1005929032764.
- (25) Iiyama, I.; Hasegawa, S. In situ CO₂ profiles with complementary monitoring of O₂ in a drained peat layer. *Soil Sci. Plant Nutr.* **2009**, *55*, 26–34, DOI: 10.1111/j.1747-0765.2008.00331.x.
- (26) Fenner, N.; Freeman, C.; Lock, M. A.; Harmens, H.; Reynolds, B.; Sparks, T. Interactions between elevated CO₂ and warming could amplify DOC exports from peatland catchments. *Environ. Sci. Technol.* **2007**, *41*, 3146–3152, DOI: 10.1021/es061765v.
- (27) Tanaka, N.; Yutani, K.; Aye, T.; Jinadasa, K. B. S. N. Effect of broken dead culms of *Phragmites australis* on radial oxygen loss in relation to radiation and temperature. *Hydrobiol.* **2007**, *583*, 165–172, DOI: 10.1007/s10750-006-0483-7.
- (28) Brix, H.; Lorenzen, B.; Morris, J. T.; Schierup, H. H.; Sorrell, B. K. Effect of oxygen and nitrate on ammonium uptake kinetics and adenylate pools in *Phalaris arundinacea* L. and *Glyceria maxima* (Hartm) Holmb. *Proc. R. Soc. Edinburgh* **1994**, *102B*, 333–342.
- (29) Kercher, S. M.; Zedler, J. B. Flood tolerance in wetland angiosperms: A comparison of invasive and noninvasive species. *Aquat. Bot.* **2004**, *80*, 89–102, DOI: 10.1016/j.aquabot.2004.08.003.
- (30) Askaer, L.; Elberling, B.; Jørgensen, C. J.; Friberg, T.; Hansen, B. U. Plant-mediated CH₄ transport and C gas dynamics quantified in situ in a *Phalaris arundinacea*-dominant wetland. *Plant Soil* **2011**, DOI: 10.1007/s11104-011-0718-x.